University of Birmingham
Research at Birmingham

The structural and functional connectivity of the posterior cingulate cortex : comparison between deterministic and probabilistic tractography for the investigation of structure–function relationships

Khalsa, Sakh; Mayhew, Stephen D.; Chechlacz, Magdalena; Bagary, Manny; Bagshaw, Andrew P.

DOI:
10.1016/j.neuroimage.2013.12.022

License:
Creative Commons: Attribution (CC BY)

Document Version
Publisher's PDF, also known as Version of record

Citation for published version (Harvard):
Khalsa, S, Mayhew, SD, Chechlacz, M, Bagary, M & Bagshaw, AP 2014, 'The structural and functional connectivity of the posterior cingulate cortex : comparison between deterministic and probabilistic tractography for the investigation of structure–function relationships', *NeuroImage*, vol. 102, pp. 118-127. https://doi.org/10.1016/j.neuroimage.2013.12.022

Link to publication on Research at Birmingham portal

Publisher Rights Statement:
Eligibility for repository : checked 3/11/2014

General rights
Unless a licence is specified above, all rights (including copyright and moral rights) in this document are retained by the authors and/or the copyright holders. The express permission of the copyright holder must be obtained for any use of this material other than for purposes permitted by law.

•Users may freely distribute the URL that is used to identify this publication.
•Users may download and/or print one copy of the publication from the University of Birmingham research portal for the purpose of private study or non-commercial research.
•User may use extracts from the document in line with the concept of 'fair dealing' under the Copyright, Designs and Patents Act 1988 (?)
•Users may not further distribute the material nor use it for the purposes of commercial gain.

Where a licence is displayed above, please note the terms and conditions of the licence govern your use of this document.

When citing, please reference the published version.

Take down policy
While the University of Birmingham exercises care and attention in making items available there are rare occasions when an item has been uploaded in error or has been deemed to be commercially or otherwise sensitive.

If you believe that this is the case for this document, please contact UBIRA@lists.bham.ac.uk providing details and we will remove access to the work immediately and investigate.

Download date: 19. Apr. 2024

NeuroImage 102 (2014) 118–127

Contents lists available at ScienceDirect

NeuroImage

journal homepage: www.elsevier.com/locate/ynimg

Review

The structural and functional connectivity of the posterior cingulate cortex: Comparison between deterministic and probabilistic tractography for the investigation of structure–function relationships

Sakh Khalsa [a,b,c], Stephen D. Mayhew [a,b], Magdalena Chechlacz [d], Manny Bagary [c], Andrew P. Bagshaw [a,b,*]

[a] School of Psychology, University of Birmingham, Birmingham, UK
[b] Birmingham University Imaging Centre (BUIC), University of Birmingham, Birmingham, UK
[c] Department of Neuropsychiatry, The Barberry Centre for Mental Health, Birmingham, UK
[d] Department of Experimental Psychology, Oxford University, Oxford, UK

ARTICLE INFO

Article history:
Accepted 11 December 2013
Available online 21 December 2013

Keywords:
DMN
Diffusion tensor imaging
fMRI
Functional connectivity
Structural connectivity
Tractography
Precuneus

ABSTRACT

The default mode network (DMN) is one of the most studied resting-state networks, and is thought to be involved in the maintenance of consciousness within the alert human brain. Although many studies have examined the functional connectivity (FC) of the DMN, few have investigated its underlying structural connectivity (SC), or the relationship between the two. We investigated this question in fifteen healthy subjects, concentrating on connections to the precuneus/posterior cingulate cortex (PCC), commonly considered as the central node of the DMN. We used group independent component analysis (GICA) and seed-based correlation analysis of fMRI data to quantify FC, and streamline and probabilistic tractography to identify structural tracts from diffusion tensor imaging (DTI) data. We first assessed the presence of structural connections between the DMN regions identified with GICA. Of the 15 subjects, when using the probabilistic approach 15 (15) demonstrated connections between the PCC and mesial prefrontal cortex (mPFC), 11 (15) showed connections from the PCC to the right inferior parietal cortex (rIPC) and 8 (15) to the left IPC. Next, we assessed the strength of FC (magnitude of temporal correlation) and SC (mean fractional anisotropy of reconstructed tracts (streamline), number of super-threshold voxels within the mask region (probabilistic)). The lIPC had significantly reduced FC to the PCC compared to the mPFC and rIPC. No difference in SC strength between connections was found using the streamline approach. For the probabilistic approach, mPFC had significantly lower SC than both IPCs. The two measures of SC strength were significantly correlated, but not for all paired connections. Finally, we observed a significant correlation between SC and FC for both tractography approaches when data were pooled across PCC–lIPL, PCC–rIPL and PCC–mPFC connections, and for some individual paired connections. Our results suggest that the streamline approach is advantageous for characterising the connectivity of long white matter tracts (PCC–mPFC), whilst the probabilistic approach was more reliable at identifying PCC–IPC connections. The direct comparison of FC and SC indicated that pairs of nodes with stronger structural connections also had stronger functional connectivity, and that this was maintained with both tractography approaches. Whilst the definition of SC strength remains controversial, our results could be considered to provide some degree of validation for the measures of SC strength that we have used. Direct comparisons of SC and FC are necessary in order to understand the structural basis of functional connectivity, and to characterise and quantify the changes in the brain's functional architecture that occur as a result of normal physiology or pathology.

© 2014 Elsevier Inc. All rights reserved.

Contents

* Corresponding author at: University of Birmingham, School of Psychology, Edgbaston B15 2TT, UK.
E-mail address: a.p.bagshaw@bham.ac.uk (A.P. Bagshaw).

1053-8119/$ – see front matter © 2014 Elsevier Inc. All rights reserved.
http://dx.doi.org/10.1016/j.neuroimage.2013.12.022

Introduction

The human brain is organised into a series of functional networks that exhibit correlations in activity between individual regions even in the absence of stimulation (Biswal et al., 1995; Gusnard et al., 2001; Raichle et al., 2001; Shulman et al., 1997). This resting-state activity can be measured from low frequency fluctuations in the blood oxygen level dependent (BOLD) fMRI signal (Biswal et al., 1995). One of the most studied resting-state networks (RSNs) is the default mode network (DMN) (Greicius et al., 2003; Horovitz et al., 2009; Raichle et al., 2001; Shulman et al., 1997) consisting of the posterior cingulate/precuneus cortex (PCC), the left inferior parietal cortex/angular gyrus (lIPC), the right inferior parietal cortex/angular gyrus (rIPC) and the medial prefrontal/anterior cingulate cortex (mPFC). Many studies have investigated the functional connectivity (FC) of the DMN (Damoiseaux and Greicius, 2009; Greicius et al., 2003; Gusnard et al., 2001; Raichle et al., 2001; Shulman et al., 1997). However, the structural connectivity (SC) that ultimately provides the anatomical substrate for functional interactions, and the relationship between FC and SC, is less well understood.

SC can most readily be defined non-invasively using diffusion-tensor imaging (DTI) approaches allied with tractography analysis. DTI allows the tracking of white-matter pathways by measuring the fractional anisotropic diffusion (FA) of water molecules along neuronal axon fibres (Basser and Le Bihan, 1992; Basser et al., 1994; Hagmann et al., 2003; Mori and Zhang, 2006). Whilst a number of different tractography algorithms of varying complexity exist, the two main distinguishing factors relate to how white matter tracts are modelled within a voxel (i.e. a single or multiple fibre orientations) and how the tracts are reconstructed (i.e. interpolated streamlines or probabilistic global connectivity estimations). These choices can have a profound effect on the estimated white matter fibre tracts, and hence on the judgement of whether two brain regions are structurally connected (Yo et al., 2009). The question of how SC underpins and constrains FC, and the extent to which the underlying SC is responsible for the maintenance and regulation of FC, remains unclear. The examination of structure–function relationships in human neuroimaging data is a burgeoning field (Damoiseaux and Greicius, 2009; Guye et al., 2008), not least because it may provide a way of understanding the modifications in FC that have been observed in many neurological and psychiatric disorders (Broyd et al., 2009). The added value of investigating the relationship between SC and FC has recently been highlighted in patients with idiopathic generalised epilepsy (Zhang et al., 2011) and traumatic brain injury (Kinnunen et al., 2011).

Several studies have investigated structure–function relationships in a variety of brain networks, and taken together this work displays general agreement that functionally connected regions are also structurally connected (Greicius et al., 2009; Hagmann et al., 2007; Honey et al., 2009; Johansen-Berg et al., 2004; Mars et al., 2010, 2011; Skudlarski et al., 2008; van den Heuvel et al., 2009; Zhang et al., 2010). However, the related question of whether regions that are more strongly functionally connected (i.e., a higher correlation coefficient between paired functional time series) are also more strongly structurally connected has received less attention (but see Skudlarski et al., 2008). One of the reasons for this is that whilst a higher correlation between fMRI time series, after removal of physiological, scanner and movement confounds, provides a measurement of stronger FC, inferring the 'strength' of SC from metrics that can be extracted from existing diffusion weighted scans, such as fractional anisotropy (FA) or a probabilistic connectivity score, is considerably more difficult. As discussed in detail by Jones et al. (2013) diffusion weighted imaging (DWI) provides information about the directionality of water diffusion within the macroscopic volumes that are sampled in typical voxels. With certain assumptions (e.g., the fitting of voxel-wise single tensor models in the simplest case), preferred diffusion directions can be identified, and tractography algorithms can subsequently be used to estimate the likelihood of the existence of connections between two regions. However, there remains considerable controversy over the extent to which variation in structural connectivity metrics can be interpreted as indexing variations in the strength of those structural connections (i.e., is a higher FA indicative of an increased strength of SC?), since there are contributions from several methodological and physiological factors which are not related to the underlying connectivity (Jbabdi and Johansen-Berg, 2011; Jones et al., 2013). Indeed, at the macroscopic level assessed by DWI, and in the absence of precise and validated markers of specific aspects of the underlying physiology (e.g., myelination), there is ambiguity about the very definition of 'strength' of structural connectivity from DWI data. Whilst it is clear that there are several potential contributions to variation in DWI metrics, it seems a plausible hypothesis that at least part of that variance can be attributed to underlying differences in SC strength, with 'strength' defined in the broadest sense and recognised as a concept that requires further physiological clarification. One way of testing this hypothesis is by direct comparison with the strength of FC. Considering the potential sources of variability in DWI metrics, a correlation between FC and a particular DWI metric would only be expected if the metric coded for variations in underlying SC strength.

In the current study we focused on the DMN as one of the most reliably detected RSNs, whose spatiotemporal pattern of activity has been observed to be altered in a range of neurological and psychiatric disorders (Broyd et al., 2009), as well as during altered states of consciousness such as sleep (Horovitz et al., 2009; Sämann et al., 2010), coma (Norton et al., 2012) and anaesthesia (Fiset et al., 1999). Few studies have investigated the SC of the DMN (Greicius et al., 2009; Hagmann et al., 2008; Skudlarski et al., 2008; van den Heuvel et al., 2009), and some uncertainty remains concerning the existence of connections between the PCC and inferior parietal cortices (Greicius et al., 2009), potentially because of problems related to crossing fibres and the choice of tractography approaches (Yo et al., 2009).

We used group independent component analysis (GICA) to spatially identify the DMN from resting-state fMRI data. We subsequently defined the PCC, the core node of the DMN (Hagmann et al., 2008; Leech et al., 2011, 2012), as the seed region from which to assess SC and FC to the three other principle nodes of the DMN (mPFC and bilateral IPC). SC was defined using two tractography algorithms, interpolated streamline (Conturo et al., 1999) and probabilistic global connectivity estimation (Behrens et al., 2003; Hagmann et al., 2003) to investigate whether different analysis methods can lead to different conclusions regarding the relationship between SC and FC.

The study tested four hypothesis: i) the PCC is structurally connected to the other nodes of the DMN, ii) for a given pair of DMN nodes the strength of FC between those nodes is mirrored by the strength of SC, iii) FC and SC are correlated across the nodes of the DMN, and iv) the FC–SC relationships identified are not affected by the definition of SC.

Methods and materials

Subjects

DTI and fMRI data were acquired from fifteen healthy adults (right handed, 10 females, 23–29 years old, mean age = 24.6 years) using a 3 Tesla Philips Achieva MRI scanner at Birmingham University Imaging Centre (BUIC), University of Birmingham. Participants had no history of any neurophysiological, neuropsychological or neurological illness. Written informed consent was obtained from all participants, and the study was approved by the University of Birmingham Ethics Committee.

Image acquisition and preprocessing

All subjects were scanned in a single session without changing their position and were instructed to lie still in the scanner and relax with eyes open. All participants confirmed that they remained awake and alert through the scanning session. Each subject underwent one resting-state fMRI scan of 5 min duration, with the following parameters: 150 dynamics, repetition time (TR) = 2000 ms, echo time (TE) = 35 ms, flip angle = 80°, voxel size $3 \times 3 \times 4$ mm^3, and 32 slices. In addition, they underwent a 13 minute echo planer DTI scan: TR = 5191 ms, TE = 77 ms, field of view (FOV) = $224 \times 150 \times 224$ mm, angulation = 0°, and voxel size 2 mm isotropic. A total of 75 slices were acquired for b values of b = 0 and b = 1500 mm^2/s obtained by applying gradients along 61 different diffusion directions. Additionally, a high-resolution (1 mm isotropic) T1-weighted anatomical image was acquired in each subject.

Pre-processing of the fMRI data was performed using FSL, the FMRIB Software Library (http://www.fmrib.ox.ac.uk/fsl, Smith et al., 2004). The following procedures were applied: motion correction (Jenkinson et al., 2002) using MCFLIRT, slice timing correction, spatial smoothing using a Gaussian kernel (FWHM = 6 mm) and a high-pass filter cutoff at 100 s ($f > 0.01$ Hz).

DTI scans were pre-processed using the FSL Brain Extraction Tool (BET, Behrens et al., 2003) for skull stripping and the FSL Diffusion Toolkit (Smith et al., 2004) to minimise eddy current distortion effects and for registration of the diffusion volumes.

Defining Regions of Interest (ROI) from functional scans

All fMRI data were registered to MNI standard space and temporally concatenated across subjects. To identify the DMN, GICA was then performed using MELODIC (Beckmann et al., 2005). The number of output components was set to 10, in accordance with a recent study (Schopf et al., 2010) and in the absence of a clear consensus as to the optimum number of components. A low dimensionality reduction ensures that the DMN will be decomposed into a single component, which makes its identification more straightforward. A single independent component representing the DMN was identified by visual inspection from its characteristic spatial map. The DMN Z-statistical map was then thresholded at Z = 4 and manually divided into four group-space ROIs: PCC, mPFC and left and right IPC. We focused on these four ROIs as they have been consistently reported as constituting robust regions of the DMN (Damoiseaux and Greicius, 2009; Greicius et al., 2003; Horovitz et al., 2009; Raichle et al., 2001). Other brain regions (e.g., hippocampus, parahippocampal gyrus) have been observed, but are less consistently reported.

Measuring DMN FC

Seed-based functional connectivity analysis was performed (Fox et al., 2005) using in-house MATLAB code (MathWorks, USA). The preprocessed functional data was further filtered ($0.009 < f < 0.08$ Hz) and single voxel co-ordinates taken from each subject's individual functional scan for regions of white matter and ventricles. The white matter and ventricular signals, the global brain signal and the motion parameters were removed from the data using linear regression. The PCC ROI was then used as the seed to measure the strength of FC to all other DMN ROIs. The BOLD timeseries within a $3 \times 3 \times 3$ voxel cube, centred on the peak Z-statistic voxel in the PCC, was averaged and correlated with all other brain voxels. This produced a whole-brain map of Pearson's correlation coefficients which allowed FC between regions of the DMN to be assessed and quantified. FC was defined for the following pairs of ROIs: PCC to mPFC, PCC to lIPC and PCC to rIPC, by averaging the voxel-wise correlation coefficients within a $3 \times 3 \times 3$ voxel cube centred on the maximum Z-statistic voxel within each target ROI.

Measuring DMN SC

In order to investigate SC of the DMN, each group-space ROI was co-registered to each individual's native DTI data space using FLIRT (Jenkinson et al., 2002). DMN ROIs were then binarised and registered to the b0 volume of each subject. This allowed tractography to be performed to determine whether these functionally connected regions were also structurally connected.

Interpolated streamline tractography

The interpolated streamline algorithm (Basser and Le Bihan, 1992; Conturo et al., 1999) was used to estimate fibre tracts between ROIs. Using FMRIB's diffusion toolbox (FDT v2.0, http://fsl.fmrib.ox.ac.uk/fsl/fslwiki/FDT), DTIFIT was used to fit a single tensor model at each voxel of the preprocessed eddy current corrected diffusion weighted data. Tractography was carried out using the Diffusion Toolkit (DTK) and tracts reconstructed using Trackvis (http://www.trackvis.org/). Tracts were considered as connecting ROIs if any part of them passed through the ROI en route to other cortical regions. Path tracing was permitted to continue until the FA fell below 0.2 or until the maximum angle between path segments was larger than 35° (Johansen-Berg et al., 2004). As well as using visual confirmation of the existence of SC, reconstructed tracts were identified using a white matter atlas (Mori et al., 2011) and mean FA values of structural connections were used as an indicator of the strength of structural connections between nodes (Ben-Shachar et al., 2007; Bozzali et al., 2005).

Probabilistic tractography

Probabilistic tractography was performed using FMRIB's diffusion toolbox (FDT v2.0, http://fsl.fmrib.ox.ac.uk/fsl/fslwiki/FDT). BEDPOSTX was used to model 5000 iterations within each voxel with a curvature threshold of 0.2, a step length of 0.5 and a maximum number of 2000 steps (Behrens et al., 2007). Target masks were used (mPFC, lIPC and rIPC) and a distribution of fibre orientations was calculated between pairs of masks using the PCC as a seed mask (i.e. PCC–rIPC, PCC–lIPC, PCC–mPFC). The connection probability was given by the number of tracts that reached a target voxel (in the target mask) from a given seed voxel (from the seed mask). This is an estimate of the most likely location and strength of a pathway between the two areas (Behrens et al., 2007). Thresholding of probabilistic tractography remains an unsolved statistical issue (Morris et al., 2008). We used FSLstats to identify the voxel with the maximum connectivity value within the connectivity distribution map of each participant and used thresholds to 50%, 25% and 15% of the maximum connectivity value to determine the optimum threshold value (i.e. keeping all other voxels which had values more than 15%, 25% or 50% of the maximum connectivity value, Bennett et al., 2011).

Comparison of structure and function

We assessed the nature of the link between the two measures of SC and between structural and functional connectivity in three ways: 1) structural pairwise connections were identified between the PCC and each node of the DMN as being either present or absent, by visual inspection of connections between nodes, 2) the strength of connection to the PCC from each of the other three nodes of the DMN was determined separately for FC and the two methods of quantifying SC. Those subjects who did not demonstrate pairwise structural connections for a given pair of nodes were excluded from this analysis, 3) the degree of SC–FC coupling was determined by linear correlation analysis for each pairwise connection between nodes, and for the DMN as a whole (i.e., including all pairs together).

Statistical analysis

For FC and SC separately (i.e., comparison 2 above) we compared the FC and SC between the three pairs of ROIs (PCC–mPFC, PCC–lIPC, PCC–rIPC) using repeated measures one-way ANOVA (SSPS Inc., Chicago USA). Secondly, bivariate correlation analysis (SPSS Inc., Chicago USA) was carried out to determine the relationship between deterministic and probabilistic tractography, and between SC and FC (comparison 3 from Statistical analysis section), using mean FA streamline data, mean probability distribution connectivity data and mean FC correlation coefficients.

Results

Functional connectivity

A single component containing the major nodes of the DMN was identified visually from the GICA decomposition (Fig. 1). Seed-based FC was then used to measure the strength of FC for each pairwise connection between the PCC seed and the mPFC, lIPC, and rIPC. Repeated measures one-way ANOVA indicated a significant main effect of region upon FC, demonstrating differences in FC between the three pairwise connections of the DMN (i.e., PCC–mPFC, PCC–lIPC and PCC–rIPC, $F(2,28) = 3.880$, $p = 0.033$). Post-hoc T-tests indicated a significant difference in FC between PCC–mPFC and PCC–lIPC ($p = 0.023$), as well as between PCC–rIPC and PCC–lIPC ($p = 0.037$). In contrast, the FC between PCC–mPFC was not significantly different to that between PCC–rIPC ($p = 0.980$). These group data are plotted in Fig. 4a. Mean correlation coefficients (i.e. magnitude of FC) were consistent between subjects for a particular paired connection, as indicated by the relatively small standard errors. The strongest FC was measured between the PCC–rIPC (mean $R = 0.1556$) and the weakest between the lIPC–PCC (mean $R = 0.0998$), with the mPFC–PCC intermediate (mean $R = 0.1362$).

Structural connectivity: streamline tractography

All of the subjects (15/15) demonstrated clear cingulate tracts connecting the PCC to the mPFC. White matter tracts were observed to link the PCC to the rIPC in 11/15 subjects and to the lIPC in 8/15 subjects. In total 34/45 connections were detected from 15 subjects (see data in Fig. 2 and examples in Figs. 3a–f).

The strength of white matter connections was assessed by measuring the mean FA along reconstructed tracts. Although SC assessed by streamline tractography showed a similar pattern to the FC in terms of the relative strengths between the different nodes (Fig. 4b), no significant main effect of region upon SC was detected ($F(2,14) = 0.752$, $p = 0.414$).

Structural connectivity: probabilistic tractography

For the probabilistic data, SC was found between the PCC and the other three nodes in all subjects (15/15 for all three pairs of ROIs leading to a total of 45 connections, see examples in Figs. 3g–i). When considering the strength of SC (number of voxels above threshold), similar to the deterministic approach the rIPC had greater connectivity than the lIPC, but in contrast the mPFC demonstrated less connectivity than both rIPC and lIPC. The pattern of SC between the pairs of nodes was comparable across all thresholds. The mean SC of the PCC to the different nodes was found to be significantly different at the 15% threshold (one-way ANOVA, $F(1,19) = 5.00$, $p = 0.029$). Post-hoc T-tests revealed differences in SC between PCC–mPFC and PCC–lIPC ($p = 0.015$) connections and also between PCC–rIPC and PCC–mPFC ($p = 0.014$) connections. The strength of SC between PCC–lIPC and PCC–rIPC was not significantly different ($p = 0.189$, Fig. 4c). At the 25% and 50% thresholds the mean SC between the PCC and the different nodes was not significantly different ($F(1,17) = 3.10$, $p = 0.90$ and $F(1,21) = 0.22$, $p = 0.74$). However, at both of these thresholds the pattern of connectivity looked qualitatively similar for the IPC regions to that at a threshold of 15% (Fig. 4c).

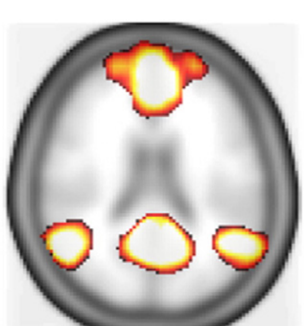

Fig. 1. The GICA map representing the DMN which was used to define ROIs for all FC and SC analyses.

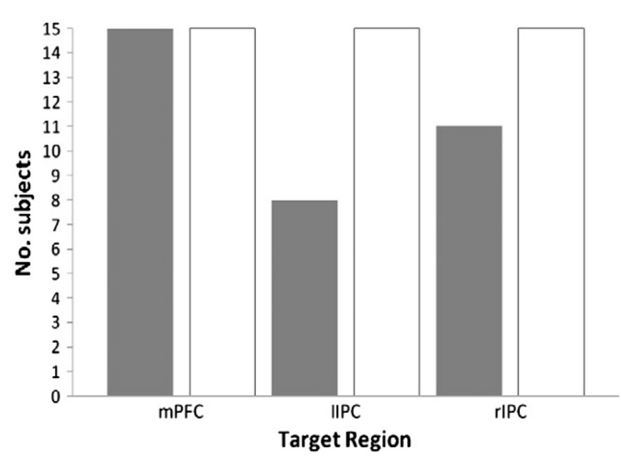

Fig. 2. The total number of subjects demonstrating SC with the PCC for each target region using deterministic streamline tractography (grey bars) and probabilistic tractography (white bars).

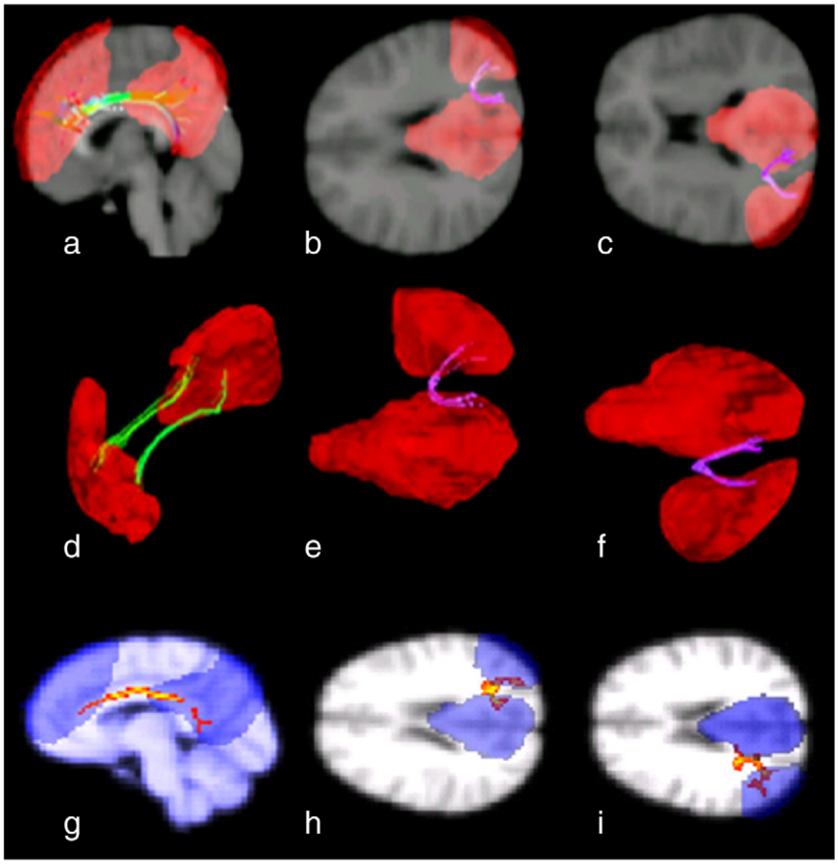

Fig. 3. An example of structural connections reconstructed using streamline tractography. The functional nodes of the DMN are shown in red. a) and d) show the cingulate tracts reconstructed between the mPFC and the PCC; b) and e) show the right angular/lateral parietal lobule white matter and precuneus/posterior cingulate white matter tracts connecting the PCC to the rIPC; c) and f) show the left angular white matter/lateral parietal lobule and precuneus/posterior cingulate white matter tracts connecting the PCC to the lIPC. In g–i the same tracts are shown reconstructed with probabilistic tractography (the functional nodes of the DMN are shown in blue and tract connection probability distribution in red/orange, the more orange/yellow the colour the greater the probability of a connection).

Relationship between deterministic and probabilistic tractography

Fig. 5 shows the relationship between deterministic and probabilistic tractography strengths (i.e., mean FA along reconstructed tracts vs number of suprathreshold voxels). Only subjects who showed both deterministic and probabilistic connections are included. Data are plotted for a probabilistic threshold of 25%, but the results were comparable for 15% and 50%. In Fig. 5a, all paired connections to the PCC across all subjects are plotted together, whilst in Figs. 5b–d the data for each of the three paired connections are plotted separately (PCC–mPFC in b, PCC–lIPC in c and PCC–rIPC in d). Only the posterior–anterior connections linking the PCC with the mPFC demonstrated a significant correlation ($R = 0.76$, $p < 0.002$). This positive correlation exists despite the fact that the probability of PCC–mPFC connections was low with probabilistic tractography, as indicated by the relatively small number of voxels above threshold.

Relationship between structure and function

Fig. 6 shows the relationship between measures of FC and SC strengths for all paired connections together (subplots a, e and i) and separately (subplots b–d, f–h, and j–l). The results for deterministic tractography are shown in the top row. The middle row (e–h) shows the results for probabilistic tractography at a threshold of 25%, restricted to those subjects who had deterministic connections to allow a direct comparison with the top row. The bottom row (i–l) again shows the probabilistic results, but with all subjects included since all subjects demonstrated some degree of connectivity with probabilistic tractography (Fig. 2).

A significant positive correlation was found between FC and SC measured by streamline tractography when pooling across all pairs of connections and all subjects (Fig. 6a, $R = 0.48$, $p = 0.005$). Considering each of the paired connections to the PCC individually, streamline tractography did not demonstrate any significant correlations between SC and FC (Figs. 6b–d, minimum p value 0.098), although there was something of a general positive trend. A similar analysis for probabilistic tractography demonstrated a significant correlation between SC and FC when all paired connections were considered, both when only those subjects who showed deterministic connections were included (Fig. 6e, $R = 0.37$, $p = 0.039$) and when all subjects were included (Fig. 6i, $R = 0.33$, $p = 0.027$). Of the paired connections to the PCC considered independently, only PCC–lIPC demonstrated a significant correlation (Fig. 6g, $R = 0.72$, $p = 0.045$, Fig. 6k $R = 0.52$, $p = 0.048$), although again there was some evidence of a general positive trend. Similar results were seen whether all subjects or only those who had deterministic connections were included. At the 15% and 50% thresholds the SC–FC correlation was found not to be significant ($R = 0.027$, $p = 0.85$ and $R = 0.031$, $p = 0.83$).

Discussion

Analysis of intrinsic functional brain activity is becoming an increasingly important and ubiquitous component of brain imaging studies. Whilst RSNs are consistently and robustly identified (Anderson et al., 2011; Damoiseaux and Greicius, 2009; Smith et al., 2009), considerable inter-individual variability exists in the strength of these RSNs. The reasons for this remain unclear, as do the causes of alterations in RSNs that have been observed in various patient populations compared to healthy

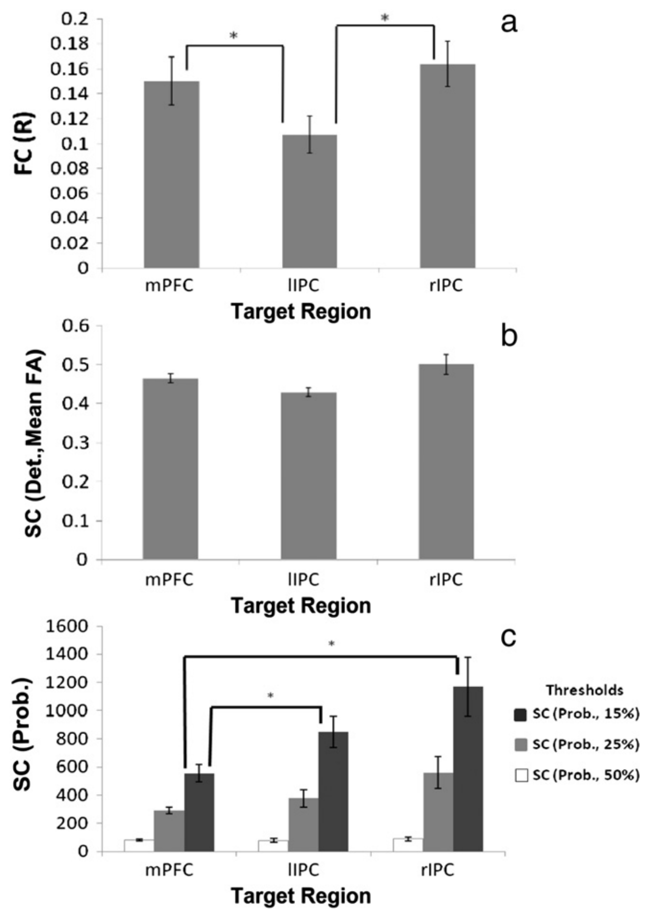

Fig. 4. Overview of SC and FC for each pairwise connection between the PCC seed and the mPFC, lIPC, and rIPC. a) Functional connectivity: group mean Pearson's correlation coefficients. b) Structural connectivity: streamline tractography. Mean FA values as a measure of structural connectivity. c) Structural connectivity: probabilistic tractography. The total number of activated voxels within the probability connectivity distribution. The three bars for each target region represent the number of activated voxels at each of the thresholds tested (15%, 25%, 50%). In all cases, error bars represent standard error. (* denotes significant difference, $p < 0.05$).

controls (Andrews-Hanna et al., 2007; Rombouts et al., 2005). One factor that is likely to contribute is individual variations in the nature and strength of the structural connectivity underlying RSNs. This aspect has received much less attention than characterising functional connectivity itself, and the current study aimed to compare two common approaches for quantifying SC and their relationship with conventional seed-based FC. We concentrated on the default mode network (DMN), and in particular on connections to the posterior cingulate/precuneus cortex (PCC), as previous work suggests that it represents the core DMN node (Hagmann et al., 2008; Leech et al., 2011, 2012) with particular relevance for the maintenance of the conscious state (Cavanna, 2007; Cavanna and Trimble, 2006). A better understanding of PCC functional and structural connectivity could thus help in understanding the physiological and pathological alterations of consciousness, such as in sleep, epilepsy, and non-epileptic attacks (Bagshaw and Cavanna, 2013).

This study improves our understanding of the relationship between structural and functional connectivity in several ways. Perhaps most importantly, it demonstrates a direct correlation between the strength of SC and the strength of FC, as well as between the two measures of SC strength defined from deterministic and probabilistic tractography (Figs. 5 and 6). This indicates that as well as the previously reported observation that regions that are functionally connected tend to be structurally connected (Hagmann et al., 2008; Honey et al., 2009; Margulies et al., 2009), there is a specific and graded relationship whereby regions which have stronger structural connections also have stronger functional signal coherence. This issue has received much less attention, partly because of the difficulty in defining the strength of SC. Skudlarski et al. (2008) noted an approximately linear relationship between resting state functional connectivity and anatomical connectivity determined from a deterministic tractography algorithm (Fiber Assignment by Continuous Tracking (FACT), Mori et al., 1999), but the definition of SC strength remains a controversial issue. Metrics that are commonly used to infer the presence of white matter connections (e.g., fractional anisotropy, probabilistic score) are not necessarily good indicators of the strength of SC, since their magnitudes may be influenced by a number of methodological and physiological factors which are not related to the underlying connectivity (Jbabdi and Johansen-Berg, 2011; Jones et al., 2013). This clear need for caution and the ambiguity surrounding the interpretability of measures of SC strength require theoretical, methodological and empirical investigation and validation.

The results presented here lead to a number of observations which are relevant to this issue. Firstly, Fig. 4 demonstrates an asymmetry between functional connections from the PCC to the left and right IPC, with higher connectivity for the right compared to the left. This functional asymmetry is mirrored in the two measures of connectivity strength derived from deterministic (mean FA along reconstructed tracts) and probabilistic (number of voxels above threshold) tractography. Secondly, the two measures of SC strength were significantly correlated (Fig. 5), but not for all paired connections. This presumably relates to the differential ability of the algorithms to cope with crossing fibres, as discussed in more detail below. Thirdly, when pooling across all paired connections, and in some cases when considering individual paired connections, strength of SC was significantly correlated with strength of FC (Fig. 6). Given the different pulse sequences used to acquire the data from which FC and SC strengths were measured, and that the definition of FC strength is much less ambiguous than for SC, these observations could be considered to provide some degree of validation for these measures of SC strength. If nothing else, the results indicate that there is some shared variance between FC and SC strengths which requires further investigation.

The first hypothesis of this study was that the PCC had direct structural connections to the other nodes of the DMN. We observe that, in general, the DMN has reasonably clear and consistent SC, and this conclusion is reached using either tractography algorithm (Figs. 2 and 3). Structural connections via cingulate tracts were found between the mPFC and PCC in all subjects for both streamline and probabilistic analyses. This is consistent with previous studies that also report robust SC between the mPFC and PCC using streamline tractography (Greicius et al., 2009; Hagmann et al., 2008; Van den Heuvel et al., 2009).

Examination of SC between the PCC and the bilateral IPC is complicated by the crossing fibre tracts of the anterior to posterior superior longitudinal fasciculus and the superior to inferior corona radiata tracts that separate them (Dougherty et al., 2005). This is likely to be a particular problem for single tensor streamline tractography (Mori and Zhang, 2006). Greicius et al. (2009) did not examine these connections, as their preliminary data showed PCC–IPC SC in only 4/23 subjects. They therefore felt that the investigation of the SC between these regions was severely restricted due to their tractography algorithm being unable to resolve the problem of crossing fibres (Greicius et al., 2009). Hagmann et al. did find evidence of structural connectivity between the PCC and the IPC regions, although this was less consistent than the PCC–mPFC (Hagmann et al., 2008). Van den Heuvel et al. used the mPFC as the seed region for their study, and therefore did not examine the connections from the PCC to the IPC (Van den Heuvel et al., 2009). Margulies et al. (2009) compared the functional connectivity of both human and macaque monkey brains against classical and recent anatomical studies. They identified a central zone of the PCC which demonstrated strong functional connectivity with the posterior part of the inferior parietal lobule and adjacent superior temporal sulcus in the macaque monkey (this corresponds in human brain to the morphology of the angular gyrus/IPC). Margulies et al. (2009) found that the functional

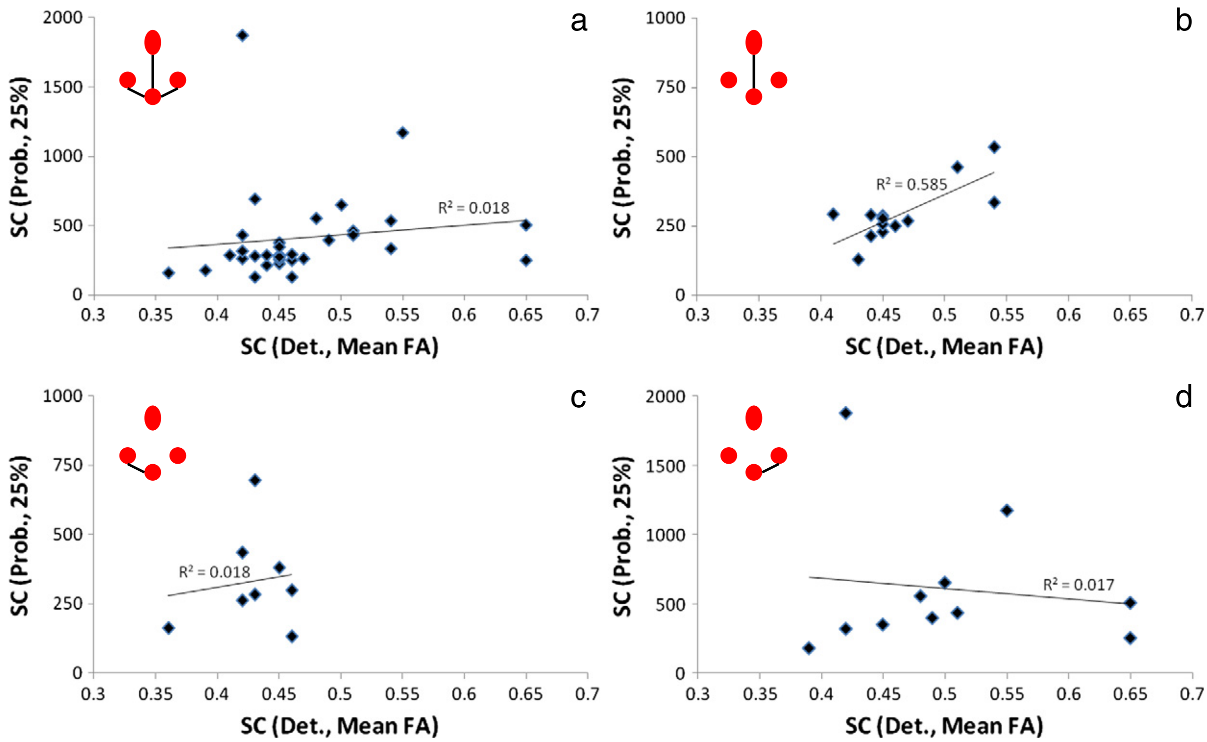

Fig. 5. Comparison between measures of SC derived from deterministic and probabilistic tractography. a) Mean FA from streamline tractography versus number of suprathreshold voxels (25% threshold) from probabilistic tractography for all paired connections pooled together. The same comparison is shown for the individual paired connections in panels b–d (i.e., b) PCC–mPFC, c) PCC–lIPC and d) PCC–rIPC). Subjects who did not show a deterministic structural connection are omitted.

connectivity patterns were remarkably consistent between species and with predictions from previous tract tracing anatomical studies in the macaque.

In the current study, structural connections between the PCC and the bilateral IPC were seen for both tractography approaches, although they were more consistent when using probabilistic tractography. The probabilistic tractography identified connections between the PCC and all other nodes of the DMN (mPFC, lIPC, rIPC) in all subjects. This finding suggests that the probabilistic approach is more effective at determining the underlying connections between regions where considerable fibre cross over is apparent (Behrens et al., 2007; Hagmann et al., 2007, 2008; Honey et al., 2009; Yo et al., 2009). However, a marked reduction in the PCC–mPFC SC was found when using probabilistic tractography (Fig. 4c). This finding suggests that the probabilistic approach is not as effective in reconstructing long pathways as streamline tractography (Fig. 4c). A degree of uncertainty in fibre orientation is apparent when pathways are reconstructed, and as the probability connectivity distribution is propagated, this uncertainty results in a decrease in the connection probability with increasing tract length. Consequently, long range connections are more difficult to characterise and have lower probability values. This effect has been previously reported, with probabilistic tractography demonstrating weaker SC with increasing tract length (Morris et al., 2008). For example, long tracts have been found to be weaker using probabilistic algorithms compared to streamline methods (Yo et al., 2009). This finding is consistent with our results (cf Figs. 4b and c).

The second hypothesis of this study was that variations in FC of the ROIs are mirrored by between ROI variations in SC. The rIPC demonstrated the strongest FC to the PCC, whilst the weakest FC was demonstrated by the lIPC (Fig. 4a). These findings show similarities with those of Horovitz et al., 2009, who found the strongest FC for the rIPC and weakest for the lIPC when using a PCC seed. A recent magnetoelectroencephalography (MEG) study (de Pasquale et al., 2012) recorded neuromagnetic signals from the DMN and several other RSNs and found that the lIPC demonstrated marked cross correlation with the dorsal attention network (DAN). This may possibly account for the reduced correlation between the lIPC and PCC in our study, by suggesting that the lIPC is a less consistent member of the DMN.

Given this asymmetry in the FC of the IPCs, and the evidence for non-DMN connectivity of the lIPC, we would expect an asymmetry in the SC of the IPCs. For each tractography algorithm there were two measures of SC, the strength of connections (mean FA for streamline data or number of activated voxels for probabilistic data) and the number of subjects who demonstrated a particular connection. We found a similar pattern for SC to that found for FC for both tractography algorithms and both measures of SC that came from them when considering the IPC regions. Our findings are consistent with previous work that suggested that regions exhibiting strong SC also exhibit strong FC, and lend weight to the idea that FC is constrained by SC (Hagmann et al., 2008; Honey et al., 2009).

The third hypothesis of this study was that SC and FC are correlated across the nodes of the DMN. This is a more specific, though more controversial as discussed above, test of the extent to which SC and FC are linked. The correlation analysis demonstrated a significant relationship between functional connectivity and structural connectivity defined using either streamline or probabilistic tractography approaches (Fig. 6). One of the issues related to the use of probabilistic tractography is that at present there is no standard methodology for thresholding maps across subjects (Morris et al., 2008). We compared the effect of using minimum thresholds of 15%, 25% and 50% of activated voxels within the connection probability distribution. The 15%, 25% and 50% thresholds were successful in including only connections consistently observed within the DMN (Figs. 2) across subjects and allowed specific tracts between ROIs to be identified within all subjects. A significant FC–SC correlation was found only with the 25% threshold (Figs. 6e, i), but not with 15% and 50% thresholds, although the overall pattern of connectivity was seen to be preserved for the IPC regions at all thresholds (Fig. 4c). The lack of a significant FC–SC correlation as a whole at the

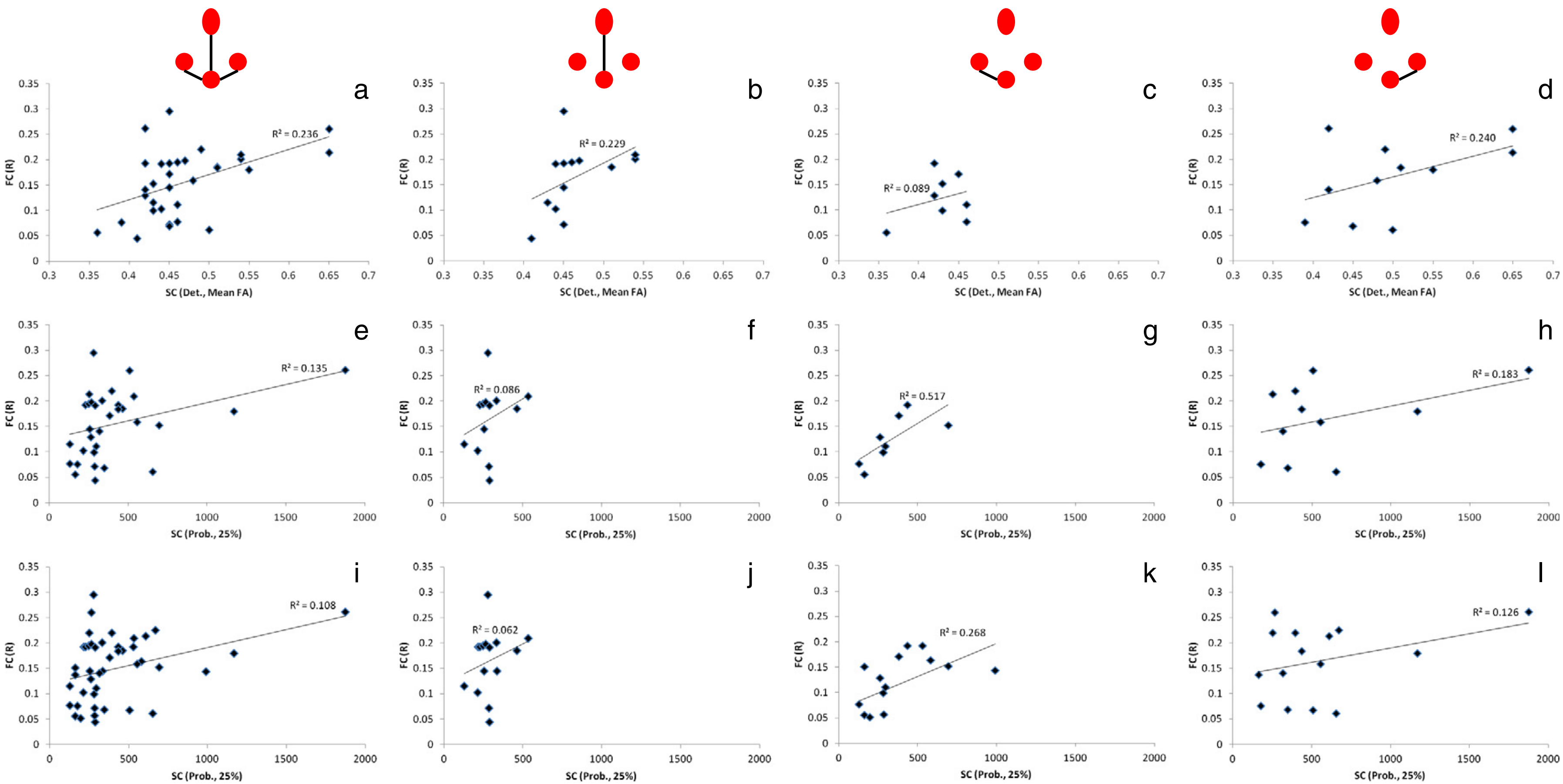

Fig. 6. Comparison between FC and SC for deterministic tractography (panels a–d) and SC for probabilistic tractography score for 25% threshold (panels e–l). Data are shown pooled across all paired connections (panels a, e, i) and for each of the paired connections separately. a–d) Functional correlation coefficient vs. mean FA along reconstructed tracts. Subjects who did not show a deterministic structural connection were omitted. e–h) FC is plotted against probabilistic SC for the same subjects shown in panels a–d. i–l) FC plotted against probabilistic SC for all subjects.

15% threshold may have been due to the significant difference in the strength of SC of the PCC–mPFC pairwise connections compared to the PCC–IPC connections.

The final hypothesis of this study was that the SC–FC relationships identified would not be dependent on the type of tractography used to define SC. As detailed above, in the majority of cases we were able to show similar relationships between FC and SC calculated using either streamline or probabilistic tractography. However, there were differences between the two tractography approaches both in terms of their definition of SC strength (Fig. 5) and their relationship with FC (Fig. 6). These differences might be related to known issues with tract reconstruction such as crossing fibres and dispersion with distance (Morris et al., 2008). It is important to consider some advantages and disadvantages of the methods. In favour of the probabilistic approach was its improved ability to cope with regions of crossing fibres, and hence to identify PCC–IPC connections more reliably than the streamline approach. However, for the anterior–posterior connections between the PCC and mPFC deterministic tractography appeared to be more related to FC than probabilistic tractography (Fig. 6). This was despite a high level of shared variance for this pair of nodes for the two structural approaches themselves (Fig. 5b). Yo et al. (2009) have found that probabilistic approaches on average produce more connected regions, but lower individual connectivity values, than streamline approaches. Accordingly, we have found that probabilistic structural connections are weaker than streamline SC when considering the mPFC–PCC pairwise connections. This suggests that streamline and probabilistic approaches may complement each other with probabilistic tractography detecting more individual connections (especially where crossover is a problem) and streamline tractography demonstrating more consistent individual strength of connectivity. In terms of understanding structure–function relationships this obviously adds a level of complexity and deserves further attention.

This study has several limitations, one of which is likely to be encountered by other studies which seek to compare explicitly the strength of SC and FC, and relates to the relationship between the regions where these quantities are calculated. Firstly, FC was quantified from a relatively small region based on the peak voxel from GICA, and would therefore primarily be in grey matter, whilst quantification of SC is obviously restricted to white matter. Secondly, the tracts we reconstructed connected the larger ROIs that represented the entire DMN nodes. The spatial group ROIs produced from the GICA analysis, whilst comparable with those from previous studies (Greicius et al., 2009; van den Heuvel et al., 2009), were much larger than the peak regions used in the FC correlation analysis, and were therefore composed of various areas of cortex. For example, the PCC ROI consisted of the precuneus, posterior cingulate and retrosplenial cortex, whilst the IPC consisted of the angular gyrus, lateral inferior parietal lobule and parts of the lateral parietal sulcus. The tracts reconstructed using the two tractography approaches demonstrated connections between the overall GICA ROIs, which included the peak FC correlation voxels. However, the tracts did not pass directly through the peak FC voxel. We therefore cannot assume SC–FC connectivity at the cytoachitectural level and studies accounting for cytoachitectural compartmentalisation may be more suited to the detailed analysis of the functional and structural characterisation of each particular region of cortex (Margulies et al., 2009). We have only addressed SC–FC at a macroscopic level, but this spatial discrepancy would be expected to reduce the observed correlation between SC and FC, meaning that the figures we have reported likely represent lower bounds on the true relationship. This study's sample size was comparable to much of the related literature, however investigating structure–function relationships in large samples such as those provided in data repositories would increase the breadth of conclusions that could be drawn. However, one of the motivations for our methodological choices was that they are readily applicable to standard clinical scanners and can therefore lay the groundwork for ongoing and future work in clinical populations and sleeping subjects. Finally, we did not investigate the effect of different preprocessing strategies on the definition of FC. Foremost amongst these is the widely utilised but much debated application of global signal regression, which can have quite a profound effect on FC, particularly in terms of inducing negative FC between networks (Fox et al., 2009; Murphy et al., 2009). However as we have focused on measuring only positive FC within a single network, the effect of global signal removal in our data is simply a reduction in FC consistent for all pairwise comparisons for a given individual. Additionally several other factors such as controlling for residual movement effects have been shown to be important to improve FC measurements in future work (Van Dijk et al., 2010, 2012). This highlights the difficulty of studying SC–FC relationships, since methodological uncertainty exists at every stage.

Our findings have demonstrated structural connections between functionally connected regions of the DMN and a significant relationship between DMN FC and SC using both deterministic and probabilistic tractography. A better understanding of how structural connections relate to functional connectivity is imperative in order to enhance our understanding of changes in SC and FC that occur as a consequence of neurological (Bozzali et al., 2005; Gattellaro et al., 2009; Kinnunen et al., 2011; Nierenberg et al., 2005; Ringman et al., 2007; Zhang et al., 2011), psychiatric (Broyd et al., 2009; Hubl et al., 2004; Li et al., 2008) and sleep (Altena et al., 2010; Nofzinger et al., 2004) disorders and whether any of these changes are reversible with therapeutic interventions.

Acknowledgments

This work was supported by the UK Engineering and Physical Sciences Research Council (grant number EP/J002909/1).

References

Altena, E., Vrenken, H., Van Der Werf, Y.D., Van den Heuvel, O.A., Van Someren, E.J.W., 2010. Reduced orbitofrontal and parietal grey matter in chronic insomnia: a voxel-based morphometric study. Biol. Psychiatry 67, 182–185.
Anderson, J.S., Ferguson, M.A., Lopez-Larson, M., Yurgelun-Todd, D., 2011. Reproducibility of single-subject functional connectivity measurements. Am. J. Neuroradiol. 32 (3), 548–555.
Andrews-Hanna, J.R., Snyder, A.Z., Vincent, J.L., Lustig, C., Head, D., Raichle, M.E., Buckner, R.L., 2007. Disruption of large-scale brain systems in advanced aging. Neuron 56 (5), 924–935.
Bagshaw, A.P., Cavanna, A.E., 2013. Resting state networks in paroxysmal disorders of consciousness. Epilepsy Behav. 26, 290–294.
Basser, P.J., Le Bihan, D., 1992. Fiber orientation mapping in an anisotropic medium with NMR diffusion spectroscopy. 11th Annual Meeting of the ISMRM, Berlin, vol. 1221 (August).
Basser, P.J., Mattiello, J., LeBihan, D., 1994. MR diffusion tensor spectroscopy and imaging. Biophys. J. 66 (1), 259–267.
Beckmann, C.F., DeLuca, M., Devlin, J.T., Smith, S.M., 2005. Investigations into resting-state connectivity using independent component analysis. Philos. Trans. R. Soc. Lond. B Biol. Sci. 360 (1457), 1001–1013.
Behrens, T.E.J., Woolrich, M.W., Jenkinson, M., Johansen-Berg, H., Nunes, R.G., Clare, S., Smith, S.M., 2003. Characterization and propagation of uncertainty in diffusion-weighted MR imaging. Magn. Reson. Med. 50 (5), 1077–1088.
Behrens, T.E.J., Berg, H.J., Jbabdi, S., Rushworth, M.F.S., Woolrich, M.W., 2007. Probabilistic diffusion tractography with multiple fibre orientations: what can we gain? Neuroimage 34 (1), 144–155.
Bennett, I.J., Madden, D.J., Vaidya, C.J., Howard, J.H., Howard, D.V., 2011. White matter integrity correlates of implicit sequence learning in healthy aging. Neurobiol. Aging 32 (12), 2317.
Ben-Shachar, M., Dougherty, R.F., Wandell, B.A., Ben-Shachar, M., Dougherty, R.F., Wandell, B.A., 2007. White matter pathways in reading. Curr. Opin. Neurobiol. 17 (2), 258–270.
Biswal, B., Yetkin, F., Haughton, V., Hyde, J., 1995. Functional connectivity in motor cortex of resting human brain using echo-planar MRI. Magn. Reson. Med. 34 (4), 537–541.
Bozzali, M., Falini, A., Cercignani, M., Baglio, F., Farina, E., Alberoni, M., Nemni, R., 2005. Brain tissue damage in dementia with Lewy bodies: an in vivo diffusion tensor MRI study. Brain 128 (7), 1595–1604.
Broyd, S.J., Demanuele, C., Debener, S., Helps, S.K., James, C.J., Sonuga-Barke, E.J., 2009. Default-mode brain dysfunction in mental disorders: a systematic review. Neurosci. Biobehav. Rev. 33 (3), 279–296.
Cavanna, A.E., 2007. The precuneus and consciousness. CNS Spectr. 12 (7), 545–552.
Cavanna, A.E., Trimble, M.R., 2006. The precuneus: a review of its functional anatomy and behavioural correlates. Brain 129 (3), 564–583.

Conturo, T.E., Lori, N.F., Cull, T.S., Akbudak, E., Snyder, A.Z., Shimony, J.S., Raichle, M.E., 1999. Tracking neuronal fiber pathways in the living human brain. Proc. Natl. Acad. Sci. 96 (18), 10422–10427.

Damoiseaux, J.S., Greicius, M.D., 2009. Greater than the sum of its parts: a review of studies combining structural connectivity and resting-state functional connectivity. Brain Struct. Funct. 213 (6), 525–533.

de Pasquale, F., Della Penna, S., Snyder, A.Z., Marzetti, L., Pizzella, V., Romani, G.L., Corbetta, M., 2012. A cortical core for dynamic integration of functional networks in the resting human brain. Neuron 74 (4), 753–764.

Dougherty, R.F., Ben-Shachar, M., Bammer, R., Brewer, A.A., Wandell, B.A., 2005. Functional organization of human occipital–callosal fiber tracts. Proc. Natl. Acad. Sci. 102, 7350–7355.

Fiset, P., Paus, T., Daloze, T., Plourde, G., Meuret, P., Bonhomme, V., Hajj-Ali, N., Beckman, S.B., Evans, A.C., 1999. Brain mechanisms of propofol-induced loss of consciousness in humans: a positron emission tomographic study. J. Neurosci. 19 (13), 5506–5513.

Fox, M.D., Snyder, A.Z., Vincent, J.L., Corbetta, M., Van Essen, D.C., Raichle, M.E., 2005. The human brain is intrinsically organized into dynamic, anticorrelated functional networks. Proc. Natl. Acad. Sci. 102 (27), 9673–9678.

Fox, M.D., Zhang, D., Snyder, A.Z., Raichle, M.E., 2009. The global signal and observed anticorrelated resting state brain networks. J. Neurophysiol. 101 (6), 3270–3283.

Gattellaro, G., Minati, L., Grisoli, M., Mariani, C., Carella, F., Osio, M., Ciceri, A.A., Bruzzone, M.G., 2009. White matter involvement in idiopathic Parkinson disease: a diffusion tensor imaging study. Am. J. Neuroradiol. 30 (6), 1222–1226.

Greicius, M.D., Krasnow, B., Reiss, A.L., Menon, V., 2003. Functional connectivity in the resting brain: a network analysis of the default mode hypothesis. Proc. Natl. Acad. Sci. 100 (1), 253–258.

Greicius, M.D., Supekar, K., Menon, V., Dougherty, R.F., 2009. Resting-state functional connectivity reflects structural connectivity in the default mode network. Cereb. Cortex 19 (1), 72–78.

Gusnard, D.A., Raichle, M.E., Raichle, M.E., 2001. Searching for a baseline: functional imaging and the resting human brain. Nat. Rev. Neurosci. 2 (10), 685–694.

Guye, M., Bartolomei, F., Ranjeva, J.P., 2008. Imaging structural and functional connectivity: towards a unified definition of human brain organization? Curr. Opin. Neurol. 21 (4), 393–403.

Hagmann, P., Thiran, J.P., Jonasson, L., Vandergheynst, P., Clarke, S., Maeder, P., Meuli, R., 2003. DTI mapping of human brain connectivity: statistical fibre tracking and virtual dissection. Neuroimage 19 (3), 545–554.

Hagmann, P., Kurant, M., Gigandet, X., Thiran, P., Wedeen, V.J., Meuli, R., Thiran, J.P., 2007. Mapping human whole-brain structural networks with diffusion MRI. PLoS One 2 (7), e597.

Hagmann, P., Cammoun, L., Gigandet, X., Meuli, R., Honey, C.J., Wedeen, V.J., Sporns, O., 2008. Mapping the structural core of human cerebral cortex. PLoS Biol. 6 (7), e159.

Honey, C.J., Sporns, O., Cammoun, L., Gigandet, X., Thiran, J.P., Meuli, R., Hagmann, P., 2009. Predicting human resting-state functional connectivity from structural connectivity. Proc. Natl. Acad. Sci. 106 (6), 2035–2040.

Horovitz, S.G., Braun, A.R., Carr, W.S., Picchioni, D., Balkin, T.J., Fukunaga, M., Duyn, J.H., 2009. Decoupling of the brain's default mode network during deep sleep. Proc. Natl. Acad. Sci. 106 (27), 11376–11381.

Hubl, D., Koenig, T., Strik, W., Federspiel, A., Kreis, R., Boesch, C., Maier, S.E., Schroth, G., Lovblad, K., Dierks, T., 2004. Pathways that make voices: white matter changes in auditory hallucinations. Arch. Gen. Psychiatry 61 (7), 658.

Jbabdi, S., Johansen-Berg, H., 2011. Tractography—where do we go from here? Brain Connect. 1 (3), 169–183.

Jenkinson, M., Bannister, P., Brady, J., Smith, S., 2002. Improved optimisation for the robust and accurate linear registration and motion correction of brain images. Neuroimage 17 (2), 825–841.

Johansen-Berg, H., Behrens, T.E.J., Robson, M.D., Drobnjak, I., Rushworth, M.F.S., Brady, J.M., Smith, S.M., Higham, D.J., Matthews, P.M., 2004. Changes in connectivity profiles define functionally distinct regions in human medial frontal cortex. Proc. Natl. Acad. Sci. 101 (36), 13335–13340.

Jones, D.K., Knösche, T.R., Turner, R., 2013. White matter integrity, fiber count, and other fallacies: the do's and don'ts of diffusion MRI. Neuroimage 73, 239–254.

Kinnunen, K.M., Greenwood, R., Powell, J.H., Leech, R., Hawkins, P.C., Bonnelle, V., Sharp, D.J., 2011. White matter damage and cognitive impairment after traumatic brain injury. Brain 134 (2), 449–463.

Leech, R., Kamourieh, S., Beckmann, C.F., Sharp, D.J., 2011. Fractionating the default mode network: distinct contributions of the ventral and dorsal posterior cingulate cortex to cognitive control. J. Neurosci. 31 (9), 3217–3224.

Leech, R., Braga, R., Sharp, D.J., 2012. Echoes of the brain within the posterior cingulate cortex. J. Neurosci. 32 (1), 215–222.

Li, W., James, G.A., Mayberg, H.S., Hu, X., 2008. Quantitative FA analysis based on VBM and probabilistic tractography connectivity between treatment-resistant patients and treatment-responsive patients with major depressive disorder. Proceedings of the International Society for Magnetic Resonance in Medicine, vol. 16, p. 2258.

Margulies, D.S., Vincent, J.L., Kelly, C., Lohmann, G., Uddin, L.Q., Biswal, B.B., Petrides, M., 2009. Precuneus shares intrinsic functional architecture in humans and monkeys. Proc. Natl. Acad. Sci. 106 (47), 20069–20074.

Mars, R.B., Sallet, J., Schüffelgen, U., Jbabdi, S., Toni, I., Rushworth, M.F., 2010. Connectivity-based subdivisions of the human right "temporoparietal junction area": evidence for different areas participating in different cortical networks. Cereb. Cortex 22 (8), 1894–1903.

Mars, R.B., Jbabdi, S., Sallet, J., O'Reilly, J.X., Croxson, P.L., Olivier, E., Noonan, M.P., Bergmann, C., Mitchell, A.S., Baxter, M.G., Behrens, T.E., Johansen-Berg, H., Tomassini, V., Miller, K.L., Rushworth, M.F., 2011. Diffusion-weighted imaging tractography-based parcellation of the human parietal cortex and comparison with human and macaque resting-state functional connectivity. J. Neurosci. 31 (11), 4087–4100.

Mori, S., Zhang, J., 2006. Principles of diffusion tensor imaging and its applications to basic neuroscience research. Neuron 51 (5), 527–539.

Mori, S., Crain, B.J., Chacko, V.P., van Zijl, P.C., 1999. Three-dimensional tracking of axonal projections in the brain by magnetic resonance imaging. Ann. Neurol. 45 (2), 265–269.

Mori, S., Oishi, K., Faria, A., van Zijl, C.M., 2011. MRI Atlas of Human White Matter, 2nd ed. Elsevier Academic Press.

Morris, D.M., Embleton, K.V., Parker, G.J., 2008. Probabilistic fibre tracking: differentiation of connections from chance events. Neuroimage 42 (4), 1329.

Murphy, K., Birn, R.M., Handwerker, D.A., Jones, T.B., Bandettini, P.A., 2009. The impact of global signal regression on resting state correlations: are anti-correlated networks introduced? Neuroimage 44 (3), 893–905.

Nierenberg, J., Pomara, N., Hoptman, M.J., Sidtis, J.J., Ardekani, B.A., Lim, K.O., 2005. Abnormal white matter integrity in healthy apolipoprotein E epsilon 4 carriers. Neuroreport 16 (12), 1369–1372.

Nofzinger, E.A., Buysse, D.J., Germain, A., Price, J.C., Miewald, J.M., Kupfer, D.J., 2004. Functional neuroimaging evidence for hyperarousal in insomnia. Am. J. Psychiatr. 161 (11), 2126–2128.

Norton, L., Hutchison, R.M., Young, G.B., Lee, D.H., Sharpe, M.D., Mirsattari, S.M., 2012. Disruptions of functional connectivity in the default mode network of comatose patients. Neurology 78 (3), 175–181.

Raichle, M.E., MacLeod, A.M., Snyder, A.Z., Powers, W.J., Gusnard, D.A., Shulman, G.L., 2001. A default mode of brain function. Proc. Natl. Acad. Sci. 98 (2), 676–682.

Ringman, J.M., O'Neill, J., Geschwind, D., Medina, L., Apostolova, L.G., Rodriguez, Y., Bartzokis, G., 2007. Diffusion tensor imaging in preclinical and presymptomatic carriers of familial Alzheimer's disease mutations. Brain 130 (7), 1767–1776.

Rombouts, S.A., Barkhof, F., Goekoop, R., Stam, C.J., Scheltens, P., 2005. Altered resting-state networks in mild cognitive impairment and mild Alzheimer's disease: an fMRI study. Hum. Brain. Mapp. 26 (4), 231–239.

Sämann, P.G., Tully, C., Spoormaker, V.I., Wetter, T.C., Holsboer, F., Wehrle, R., Czisch, M., 2010. Increased sleep pressure reduces resting-state functional connectivity. MAGMA 23 (5), 375–389.

Schopf, V., Windischberger, C., Kasess, C., Lanzenberger, R., Moser, E., 2010. Group ICA of resting—state data: a comparison. Magn. Reson. Mater. Phys. 23, 317–325.

Shulman, G.L., Fiez, J.A., Corbetta, M., Buckner, R.L., Miezin, F.M., Raichle, M.E., Petersen, S.E., 1997. Common blood flow changes across visual tasks: II. Decreases in cerebral cortex. J. Cogn. Neurosci. 9 (5), 648–663.

Skudlarski, P., Jagannathan, K., Calhoun, V.D., Hampson, M., Skudlarska, B.A., Pearlson, G., 2008. Measuring brain connectivity: diffusion tensor imaging validates resting state temporal correlations. Neuroimage 43, 554–561.

Smith, S.M., Jenkinson, M., Woolrich, M.W., Beckmann, C.F., Behrens, T.E., Johansen-Berg, H., Bannister, P.R., De Luca, M., Drobnjak, I., Flitney, D.E., Niazy, R., Saunders, J., Vickers, J., Zhang, Y., De Stefano, N., Brady, J.M., Matthews, P.M., 2004. Advances in functional and structural MR image analysis and implementation as FSL. Neuroimage 23, S208–S219.

Smith, S.M., Fox, P.T., Miller, K.L., Glahn, D.C., Fox, P.M., Mackay, C.E., Beckmann, C.F., 2009. Correspondence of the brain's functional architecture during activation and rest. Proc. Natl. Acad. Sci. 106 (31), 13040–13045.

van den Heuvel, M.P., Mandl, R.C., Kahn, R.S., Pol, H., Hilleke, E., 2009. Functionally linked resting-state networks reflect the underlying structural connectivity architecture of the human brain. Hum. Brain. Mapp. 30 (10), 3127–3141.

Van Dijk, K.R., Hedden, T., Venkataraman, A., Evans, K.C., Lazar, S.W., Buckner, R.L., 2010. Intrinsic functional connectivity as a tool for human connectomics: theory, properties, and optimization. J. Neurophysiol. 103 (1), 297–321.

Van Dijk, K.R., Sabuncu, M.R., Buckner, R.L., 2012. The influence of head motion on intrinsic functional connectivity MRI. Neuroimage 59 (1), 431–438.

Yo, T.S., Anwander, A., Descoteaux, M., Fillard, P., Poupon, C., Knösche, T., 2009. Quantifying brain connectivity: a comparative tractography study. Med. Image Comput. Comput. Assist. Interv. 886–893.

Zhang, D., Snyder, A.Z., Shimony, J.S., Fox, M.D., Raichle, M.E., 2010. Noninvasive functional and structural connectivity mapping of the human thalamocortical system. Cereb. Cortex 20 (5), 1187–1194.

Zhang, Z., Liao, W., Chen, H., Mantini, D., Ding, J.R., Xu, Q., Wang, Z., Yuan, C, Chen, G., Jiao, Q, Lu, G., 2011. Altered functional–structural coupling of large-scale brain networks in idiopathic generalized epilepsy. Brain 134 (10), 2912–2928.